RSC Advances

COMMUNICATION

View Article Online
View Journal | View Issue

Cite this: *RSC Adv.*, 2015, **5**, 10790

Cu_2O/CuO photocathode with improved stability for photoelectrochemical water reduction†

Jingfeng Han,[ab] Xu Zong,[a] Xin Zhou[a] and Can Li*[a]

Received 5th November 2014
Accepted 9th January 2015

DOI: 10.1039/c4ra13896a

www.rsc.org/advances

A p-type cuprous oxide (Cu_2O) photocathode covered with a thin layer of cupric oxide (CuO) was prepared by fast annealing of a copper foil *via* H_2–O_2 flame. The as-prepared composite photocathode is characteristic of a junction structure formed between the (110) plane of Cu_2O and the (111) plane of CuO. The Cu_2O/CuO composite photocathode showed improved stability for photoelectrochemical (PEC) water reduction by increasing the coverage of CuO on Cu_2O.

Photoelectrochemical (PEC) water splitting has aroused considerable research interest in the past decade due to its potential for converting solar energy to hydrogen fuel.[1,2] Semiconductors with suitable band gap (1.6–2.2 eV), good stability and low cost are highly desirable to make this process acceptable.[3,4] Among all the semiconductors under investigation, p-type cuprous oxide (Cu_2O) is regarded as an attractive candidate for fabricating photocathodes due to its high photoactivity and natural abundance.[5–7] The band gap of Cu_2O is *ca.* 2.1 eV, which makes it attractive for light harvesting with a theoretical photocurrent density of 14.7 mA cm^{-2} and a solar-to-hydrogen conversion efficiency of 18.7% under AM 1.5 G illumination.[8,9] However, the application of Cu_2O photocathode is limited due to the poor stability under PEC process.[6,10]

To address the above issue, surface modification has been used to protect the photoelectrode from photocorrosion in the PEC water splitting process.[11–13] For example, the stability of photoelectrode could be improved by covering conducting polymers,[14–16] metal thin films[17–19] and stable metal oxides.[13,20,21] Similar efforts have been devoted to improving the stability of Cu_2O photocathode by covering suitable metal oxide layers to prevent Cu_2O photocathode from contacting with electrolyte directly.[6] It was reported that a stable cupric oxide (CuO) layer can protect Cu_2O and provide a suitable band structure for charge transportation.[4,10,22] However, the fabrication of Cu_2O/CuO composite photocathodes is complicated and the interfacial structure between Cu_2O and CuO is unclear up to now.

Herein, we reported a facile method to prepare Cu_2O/CuO composite photocathode by heating a copper foil in H_2–O_2 flame. The photocathode is composed of internal Cu_2O layer covered with a thin layer of CuO on the external surface and the interface between Cu_2O and CuO is characteristic of a junction formed between the (110) plane of Cu_2O and the (111) plane of CuO. With the increase of CuO coverage, the Cu_2O/CuO composite photocathode showed improved stability for photoelectrochemical (PEC) water reduction.

Cu_2O/CuO composite photocathodes were prepared by heating a copper foil in a H_2–O_2 flame at *ca.* 1300 K for 2, 5, 10 or 15 s, which are denoted as HT-2S, HT-5S, HT-10S and HT-15S, respectively. The compositions of the as-prepared films were investigated by X-ray diffraction (XRD) technique (Fig. 1a). The diffraction peaks for all the prepared samples at 43.3 and 50.4 degree are indexed to the (111) and (200) plane of Cu, respectively (JCPDS card no. 04-0836). The peaks at 30.0, 36.7, 42.8, and 61.7 degree for HT-5S, HT-10S and HT-15S are the characteristic peaks of cubic phase Cu_2O (JCPDS card no. 78-2076). Meanwhile, the weak diffraction peaks at 35.8 and 39.0 degree for HT-10S and HT-15S are assigned to monoclinic CuO with the orientation of (111) plane (JCPDS card no. 48-1548). The much stronger diffraction peaks of Cu_2O compared with those of CuO indicated that Cu_2O is the dominant composition of the electrode. Moreover, the increased intensities for copper oxides indicate that the degree of copper oxidation and the crystallinity of copper oxides increase with prolonged heating duration.

The surface structure of the photocathodes was further characterized by Raman spectroscopy, which is more sensitive for investigating surface region.[23] In Fig. 1b, the Raman bands

[a]*State Key Laboratory of Catalysis, Dalian Institute of Chemical Physics, Chinese Academy of Sciences, Dalian National Laboratory for Clean Energy, Dalian 116023, China. E-mail: canli@dicp.ac.cn; Web: http://www.canli.dicp.ac.cn; Fax: +86 411 84694447; Tel: +86 411 84379070*

[b]*Graduate School of the Chinese Academy of Sciences, Beijing, 100049, China*

† Electronic supplementary information (ESI) available: Experimental details for preparation, characterization, photoelectrochemical measurement, cross-sectional SEM images and UV-visible diffuse reflectance spectra for all the samples. See DOI: 10.1039/c4ra13896a

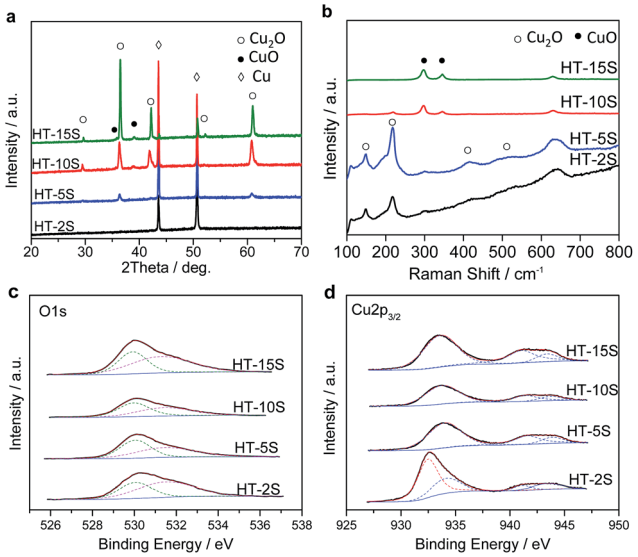

Fig. 1 XRD patterns (a), Raman spectra (b) and XPS spectra (c and d) of composite Cu_2O/CuO photocathodes.

at 154 and 218 cm^{-1} for HT-2S and HT-5S are assigned to Cu_2O.[24] The Raman bands at 292 and 324 cm^{-1} for all the samples are the characteristic bands of CuO.[25] The Raman spectra illustrate that the CuO phase exists on the surface of all the as-prepared samples and increases with prolonged heating duration. The surface compositions of samples were further investigated by X-ray photoelectron spectroscopy (XPS). Fig. 1c shows the O1s XPS spectra for the as-prepared photocathodes. All the samples exhibit a lattice O1s peak of CuO at 530.3 eV and a second peak at higher binding energy of 531.8 eV associated with the surface hydroxide.[26] For $Cu2p_{3/2}$ XPS spectra in Fig. 1d, the peak located at 932.6 eV and is assigned to $Cu2p_{3/2}$ for Cu_2O and the peak located at 933.6 eV with two satellite peaks at 944.0 and 941.2 eV is attributed to $Cu2p_{3/2}$ for CuO.[27–29] Therefore, both the CuO and Cu_2O phase were present on the surface of HT-2S, while mainly the CuO phase was present on the surface of HT-5S, HT-10S, and HT-15S. Combined with the Raman analysis, we can conclude that the surface of all the samples is covered by CuO and its thickness and coverage increase with prolonged heating duration.

Based on the analysis above, the structure of the Cu_2O/CuO composite photocathode prepared by the facile oxidation of copper foil can be confirmed. All the photocathodes were composed with low chemical oxidation state Cu_2O adjacent to the Cu substrate and high chemical state CuO layer covering the Cu_2O layer (Scheme 1). The thickness of inner Cu_2O layer and the outer CuO layer increased simultaneously as the heating process prolonged. The coverage of CuO can be increased by increasing the duration of H_2–O_2 flame heating, and a full coverage of CuO on Cu_2O was obtained for HT-10S and HT-15S.

To clarify the composite structure of as-prepared films, further investigation was conducted by the high resolution transmission electron microscopy (HRTEM) for HT-10S photocathode. Fig. 2a shows the electron diffraction of HT-10S photocathode in the selected region (inset in Fig. 2a). The diffraction mottle of Cu_2O (100) plane indicates that the Cu_2O

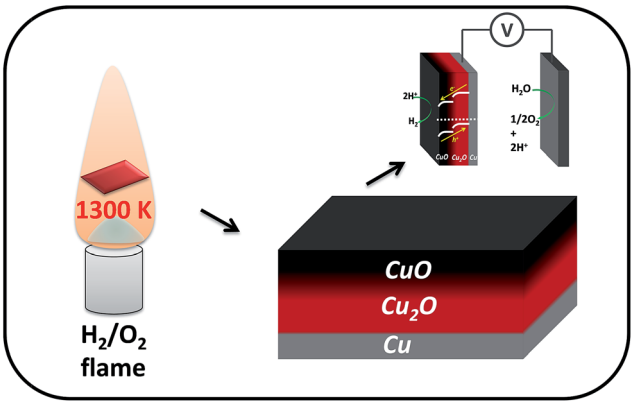

Scheme 1 Preparation and structure of Cu_2O/CuO composite photocathode in PEC water reduction reaction.

formed in this work is single crystalline in micrometre scale. Fig. 2b shows the HRTEM image of the junction region between Cu_2O and CuO. The interplanar crystal spacing of 3.0 Å and 2.34 Å is ascribed to the (110) plane of Cu_2O and (111) plane of CuO, respectively. Fig. 2c shows the HRTEM image of the exposed edge of Cu_2O. It indicates that the junction region in Fig. 2b is not formed by the treatment for HRTEM measurement. The contact between the two planes indicates the transformation from Cu_2O (110) to CuO (111), which is reasonable considering the similar surface atom arrangement (Fig. 2d).[30,31] This Cu_2O/CuO structure with high crystallinity and compact contact in junction region could be beneficial for the charge transfer and protection of Cu_2O, leading to a higher and a more stable photocurrent.[10]

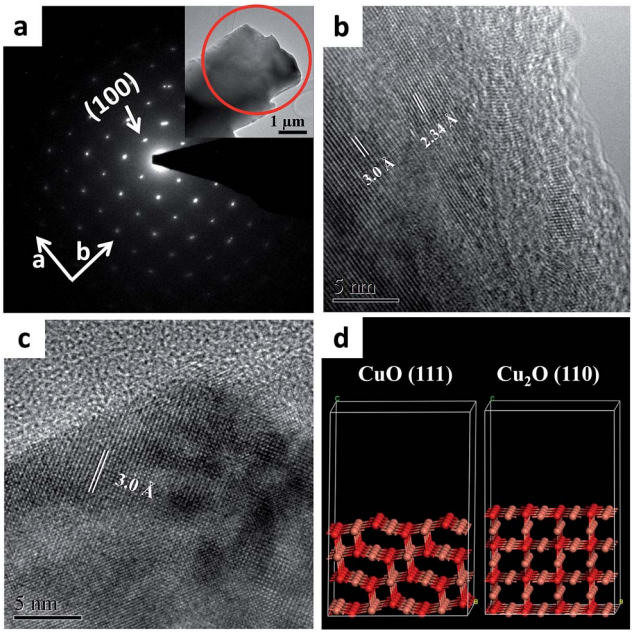

Fig. 2 The electron diffraction of HT-10S photocathode (a), the inset shows the selected region. HRTEM images of HT-10S photocathode (b and c). The surface atom arrangement of CuO (111) plane and Cu_2O (110) plane (d).

The morphologies of the as-prepared photocathodes were investigated by scanning electron microscope (SEM). As shown in Fig. 3, only small particles were found on the surface of HT-2S photocathode. When the heating duration was increased to 5 s, the small particles were agglomerated and finally formed linked and twisty nanowire network when the heating duration was increased to 10 and 15 s. According to the cross-sectional SEM images (Fig. S1†) the thickness of copper oxides of HT-5S, HT-10S and HT-15S were estimated to be *ca.* 0.26 μm, 2 μm and 3.5 μm, respectively. This also indicates that the thickness of the copper oxides increased with the prolonged heating duration, which is in good agreement with the XRD analysis. The UV-visible diffuse reflectance spectra of the photocathodes (Fig. S2†) manifest the mixed absorption properties of Cu_2O and CuO semiconductors.[32] The absorption of as-prepared samples is improved as the prolonged heating duration, which is due to the increasing amount of copper oxides.

The PEC performances of the Cu_2O/CuO composite photocathodes were evaluated at 0 V *vs.* RHE with chopped illumination under AM 1.5 G in 0.5 M Na_2SO_4 electrolyte (pH 6.82) with Ar bubbling. In Fig. 4a, the initial photocurrent densities of HT-2S, HT-5S, HT-10S and HT-15S at 0 V *vs.* RHE were −0.05, −0.11, −0.82 and −0.45 mA cm^{-2}, respectively. The improved photocurrent density for HT-10S compared with HT-2S and HT-5S could be attributed to the increase of thickness of Cu_2O oxides, which will influence the light absorption of the electrodes. The decreased current density for HT-15S compared with that for HT-10S may result from the thicker CuO layer, which will decrease the light harvesting by Cu_2O layer. Fig. 4b shows the current decay curves of as-prepared photocathodes. For HT-2S and HT-5S, the photocurrent decreased sharply to less than 20% of the initial value within 5 min. For HT-10S, the photocurrent maintains 30% of the initial value after 10 min.

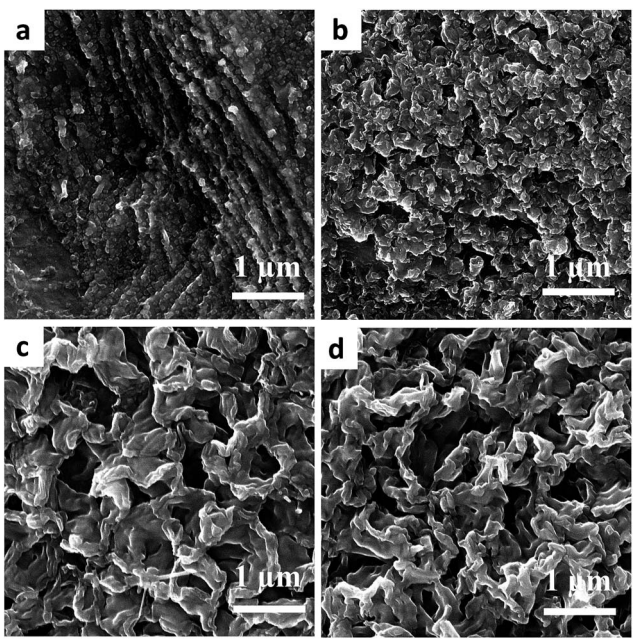

Fig. 3 SEM images of HT-2S (a), HT-5S (b), HT-10S (c) and HT-15S (d).

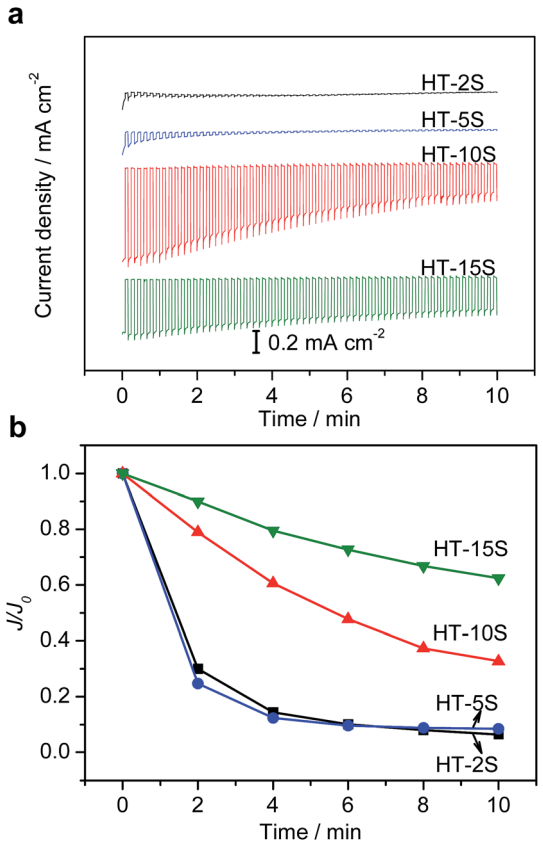

Fig. 4 Current–time curves (a) and current decay curves (b) of composite Cu_2O/CuO photocathodes. Electrolyte, 0.5 M Na_2SO_4 aqueous solution with Ar bubbling (pH 6.82); light source, AM 1.5 G (100 mW cm^{-2}) with a chopping frequency of 0.2 Hz; the potential applied for current–time test, 0 V *vs.* RHE.

The HT-15S photocathode shows a more stable photocurrent with a decrease of less than 40% for 10 min. Apparently, HT-10S and HT-15S are much more stable than HT-2S and HT-5S due to the increase of the CuO coverage. Therefore, it is evident that the as-prepared Cu_2O/CuO composite structure was beneficial for improving the stability of Cu_2O photocathode in PEC water reduction. We also note that among all the samples, HT-10S shows the highest initial photocurrent and HT-15S shows the best stability. This is reasonable considering the combined influence of CuO that will decrease the photoactivity and improve photostability of the present electrode. Therefore, CuO layer with proper thickness is desirable to balance the photoactivity and photostability in the Cu_2O/CuO composite system.

As shown in Fig. 4a, the decay of photocurrents also indicates deactivation process during PEC water reduction process, even for the relatively stable HT-15S electrode. In order to address this concern, we conducted PEC water reduction test with the participation of O_2, which was reported to have impressive effect on the cathodic current of pure Cu_2O photocathode.[33] The photocurrent and stability of HT-15S measured in air atmosphere is slightly improved compared with that in Ar atmosphere (Fig. S3†). Compared with the self-healing process observed for the $CuRhO_2$ (ref. 34) and the impressively

improved photocurrent on Cu_2O photocathodes[33] under air atmosphere, the improvement of PEC performance on HT-15S is negligible. This means that the self-healing or O_2 reduction process is negligible for the HT-15S electrode, demonstrating the reduction process from Cu_2O to Cu can be mostly prohibited by the coverage of CuO.

We then conducted PEC measurement on HT-15S in Ar atmosphere for three times. The photocurrent decayed as the PEC measurement prolonged (Fig. S4†). To understand the reason for the decay of the current, Raman spectroscopy of HT-15S electrode is measured after PEC measurement (Fig. S5†). The dominated phase for all the tested electrodes is CuO. However, the characteristic peaks of CuO for the tested electrodes get broaden and weaken and shift towards a low wavenumber compared with these for the pristine HT-15S electrode. This indicates that the crystallinity of CuO is getting worse during the PEC measurement.[35,36] In the meantime, the characteristic peak of Cu_2O appears after PEC test, manifesting the evolution of a small amount of Cu_2O with on the surface. The decreased crystallinity of CuO and the presence of Cu_2O on the electrode surface indicate that Cu(II) is transforming to Cu(I) during the PEC process. Therefore, the deactivation of as-prepared photocathode is ascribed to the reduction of CuO on the surface.

Conclusions

In summary, we presented a facile method to prepare Cu_2O/CuO composite photocathode by one-step heating treatment at *ca.* 1300 K *via* H_2–O_2 flame. The as-prepared samples consist of Cu_2O as the dominant oxide phase on the internal surface and CuO as the minor oxide phase on the external surface. The thickness of the composite oxide layers was increased by prolonging the heating duration and an intimate junction was formed between the (110) plane of Cu_2O and the (111) plane of CuO. The as-prepared composite Cu_2O/CuO photocathode shows improved PEC stability due to the protection of Cu_2O by the outer CuO layer.

Acknowledgements

This work was financially supported by 973 National Basic Research Program of the Ministry of Science and Technology (Grant 2014CB239403), National Natural Science Foundation of China (no. 21090340).

Notes and references

1 M. Gratzel, *Nature*, 2001, **414**, 338–344.
2 M. G. Walter, E. L. Warren, J. R. McKone, S. W. Boettcher, Q. X. Mi, E. A. Santori and N. S. Lewis, *Chem. Rev.*, 2010, **110**, 6446–6473.
3 Y. S. Chaudhary, A. Agrawal, R. Shrivastav, V. R. Satsangi and S. Dass, *Int. J. Hydrogen Energy*, 2004, **29**, 131–134.
4 Z. H. Zhang and P. Wang, *J. Mater. Chem.*, 2012, **22**, 2456–2464.
5 L. L. Wu, L. K. Tsui, N. Swami and G. Zangari, *J. Phys. Chem. C*, 2010, **114**, 11551–11556.
6 A. Paracchino, V. Laporte, K. Sivula, M. Gratzel and E. Thimsen, *Nat. Mater.*, 2011, **10**, 456–461.
7 K. Nakaoka, J. Ueyama and K. Ogura, *J. Electrochem. Soc.*, 2004, **151**, C661–C665.
8 A. J. Nozik, *Appl. Phys. Lett.*, 1977, **30**, 567–569.
9 A. J. Nozik and R. Memming, *J. Phys. Chem.*, 1996, **100**, 13061–13078.
10 Q. Huang, F. Kang, H. Liu, Q. Li and X. D. Xiao, *J. Mater. Chem. A*, 2013, **1**, 2418–2425.
11 Y. Nakato, A. Tsumura and H. Tsubomura, *Chem. Lett.*, 1981, **1**, 127–130.
12 F. R. F. Fan, B. L. Wheeler, A. J. Bard and R. N. Noufi, *J. Electrochem. Soc.*, 1981, **128**, 2042–2045.
13 G. J. Liu, J. Y. Shi, F. X. Zhang, Z. Chen, J. F. Han, C. M. Ding, S. S. Chen, Z. L. Wang, H. X. Han and C. Li, *Angew. Chem., Int. Ed.*, 2014, **53**, 7295–7299.
14 R. Noufi, A. J. Frank and A. J. Nozik, *J. Am. Chem. Soc.*, 1981, **103**, 1849–1850.
15 S. Mubeen, J. Lee, N. Singh, M. Moskovits and E. W. McFarland, *Energy Environ. Sci.*, 2013, **6**, 1633–1639.
16 A. Bansal and N. S. Lewis, *J. Phys. Chem. B*, 1998, **102**, 4058–4060.
17 Y. Nakato and H. Tsubomura, *J. Photochem.*, 1985, **29**, 257–266.
18 Y. Nakato, M. Hiramoto, Y. Iwakabe and H. Tsubomura, *J. Electrochem. Soc.*, 1985, **132**, 330–334.
19 B. Mei, B. Seger, T. Pedersen, M. Malizia, O. Hansen, I. Chorkendorff and P. C. K. Vesborg, *J. Phys. Chem. Lett.*, 2014, **5**, 1948–1952.
20 S. Hu, M. R. Shaner, J. A. Beardslee, M. Lichterman, B. S. Brunschwig and N. S. Lewis, *Science*, 2014, **344**, 1005–1009.
21 H. Tsubomura, Y. Nakato, M. Hiramoto and H. Yano, *Can. J. Chem.*, 1985, **63**, 1759–1762.
22 P. Wang, Y. H. Ng and R. Amal, *Nanoscale*, 2013, **5**, 2952–2958.
23 J. Zhang, Q. Xu, Z. Feng, M. Li and C. Li, *Angew. Chem., Int. Ed.*, 2008, **47**, 1766–1769.
24 A. Compaan and H. Z. Cummins, *Phys. Rev. B: Solid State*, 1972, **6**, 4753–4757.
25 Y. S. Gong, C. P. Lee and C. K. Yang, *J. Appl. Phys.*, 1995, **77**, 5422–5425.
26 S. Poulston, P. M. Parlett, P. Stone and M. Bowker, *Surf. Interface Anal.*, 1996, **24**, 811–820.
27 Z. H. Gan, G. Q. Yu, B. K. Tay, C. M. Tan, Z. W. Zhao and Y. Q. Fu, *J. Phys. D: Appl. Phys.*, 2004, **37**, 81–85.
28 Y. K. Hsu, C. H. Yu, H. H. Lin, Y. C. Chen and Y. G. Lin, *J. Electroanal. Chem.*, 2013, **704**, 19–23.
29 A. P. Chen, H. Long, X. C. Li, Y. H. Li, G. Yang and P. X. Lu, *Vacuum*, 2009, **83**, 927–930.
30 M. Altarawneh, M. W. Radny, P. V. Smith, J. C. Mackie, E. M. Kennedy, B. Z. Dlugogorski, A. Soon and C. Stampfl, *J. Chem. Phys.*, 2009, **130**, 184505.
31 V. Oison, H. Ouali, C. Lambert-Mauriat and M. Freyss, *Surf. Sci.*, 2014, **622**, 44–50.

32 S. Sunkara, V. K. Vendra, J. H. Kim, T. Druffel and M. K. Sunkara, *Catal. Today*, 2013, **199**, 27–35.
33 P. E. de Jongh, D. Vanmaekelbergh and J. J. Kelly, *J. Electrochem. Soc.*, 2000, **147**, 486–489.
34 J. Gu, Y. Yan, J. W. Krizan, Q. D. Gibson, Z. M. Detweiler, R. J. Cava and A. B. Bocarsly, *J. Am. Chem. Soc.*, 2014, **136**, 830–833.
35 T. Nikitin, R. Velagapudi, J. Sainio, J. Lahtinen, M. Räsänen, S. Novikov and L. Khriachtchev, *J. Appl. Phys.*, 2012, **112**, 094316.
36 B.-C. Yu, Y. Hwa, J.-H. Kim and H.-J. Sohn, *J. Power Sources*, 2014, **260**, 174–179.